



# Subducting oceanic high causes compressional faulting in southernmost Ryukyu forearc as revealed by hypocentral determinations of earthquakes and reflection/refraction seismic data

Yvonne Font <sup>a,\*</sup>, Serge Lallemand <sup>b</sup>

<sup>a</sup> Géosciences Azur, UMR IRD–CNRS–UPMC–UNSA 6526, 06235 Villefranche-sur-Mer, France

<sup>b</sup> Géosciences Montpellier, UMR CNRS–UM2 5243, CC.60, UM2, place E. Bataillon, 34095 Montpellier, France

## Abstract

Absolute earthquake hypocenter locations have been determined in the area offshore eastern Taiwan, at the Southernmost Ryukyu subduction zone. Location process is run within a 3D velocity model by combining the Taiwanese and neighboring Japanese networks and using the 3D MAXI technique. The study focuses on the most active seismic cluster in the Taiwan region that occurs in the forearc domain offshore eastern Taiwan. Earthquakes distribute mainly along 2 active planes. The first one aligns along the subduction interface and the second one, shallower affects the overriding margin. Focal mechanisms within the shallow group indicate that nodal planes are either compatible with high-angle back-thrusts or low-angle thrusts. The active seismic deformation exclusively indicates reverse faulting revealing that the forearc basement undergoes trench-perpendicular strong compression. By integrating the seismological image into the regional context, we favor the hypothesis in which the dense seismicity occurring offshore marks the activity of *en-échélon* high-angle reverse faults accommodating the uplift of a broken piece of Ryukyu Arc basement, called Hopping Basement Rise. The uplift is inferred to be caused by the subduction of an oceanic relief, either exotic block, seamount or oceanic crust sliver. Our favored solution satisfies the narrowness of epicenter's cluster along the Hopping Canyon, and the observation of high-angle active faults on seismic lines crossing the area. Furthermore, this solution is compatible with the active uplift of the Hopping Rise demonstrated from morphological and sedimentological data. We do not exclude the branching of the high-angle reverse faults system onto a splay fault connected with the subduction interface but further investigations are needed to map precisely the 3D distribution of active faults that break the margin.

© 2007 Elsevier B.V. All rights reserved.

**Keywords:** Splay fault; Ryukyu subduction; Taiwan; Earthquake location

## 1. Introduction

Great earthquakes mostly generate on plate interface of subduction zones. Near Taiwan, the southernmost Ryukyu subduction zone exhibits, in the Ryukyu forearc domain, the densest seismic activity of the whole area. This area, located at a few tens of kilometers from Taiwanese and Japanese coasts, has generated historical earthquakes as the June 5th 1920, magnitude-8 event (Wang and Kuo, 1995) or more recently the Mw 7.1 earthquake, on February 31st 2002 (Fig. 1 and Table 1). In this

offshore area, hypocentral determinations based on local seismological observation are usually poorly resolved. Consequently, the subduction thrust fault zone – the most destructive earthquakes and tsunamis generator – is badly imaged and seismic hazard inefficiently evaluated.

This paper reviews independent studies carried on the Nanao forearc region with the purpose of better understanding the high concentration of seismicity occurring there (Fig. 1C). We first present the morphological and tectonic structure of the southernmost Ryukyu forearc essentially based on marine reflection and refraction seismic data. In this framework, we then describe the hypocentral distribution of a refined earthquake dataset whose location has been reprocessed using appropriate heterogeneous velocity model (Font et al., 2003) and 3D location technique. We will briefly summarize the technique used to

\* Corresponding author.

E-mail addresses: [font@geoazur.obs-vlfr.fr](mailto:font@geoazur.obs-vlfr.fr) (Y. Font), [Serge.Lallemand@dstu.univ-montp2.fr](mailto:Serge.Lallemand@dstu.univ-montp2.fr) (S. Lallemand).

obtain the refined data set. More detail on the MAXI technique can be found in Font et al. (2004). Finally, this study reveals the geometry of active faults that present a potential seismogenic risk for neighboring coastal cities.

## 2. Geodynamic background

Taiwan is located at the boundary between the Philippine Sea plate (PSP) and the continental margin of the Eurasian plate (Fig. 1A). Near Taiwan, the PSP converges toward the Eurasian plate at a rate of 8–9 cm/year along N306°–N312° (Yu et al.,

1997). North-East of Taiwan, the PSP subducts beneath the rifted Eurasian plate margin (i.e. the Ryukyu Arc located south of the opening South Okinawa Trough) along the Ryukyu Trench (Fig. 1B,C). East of Taiwan, the deformed Eurasian continental margin collides against the Luzon volcanic arc, originated from the Manila east-dipping subduction system (southwest of Taiwan). The Taiwan orogen is often regarded as the result of this active collision (e.g. Suppe, 1981; Ho, 1986).

Due to the Okinawa Trough extension (Sibuet et al., 1995, 1998), the westernmost Ryukyu Arc segment is presently moving southward, 1.4 cm/year faster than NE Taiwan (Fig. 1;

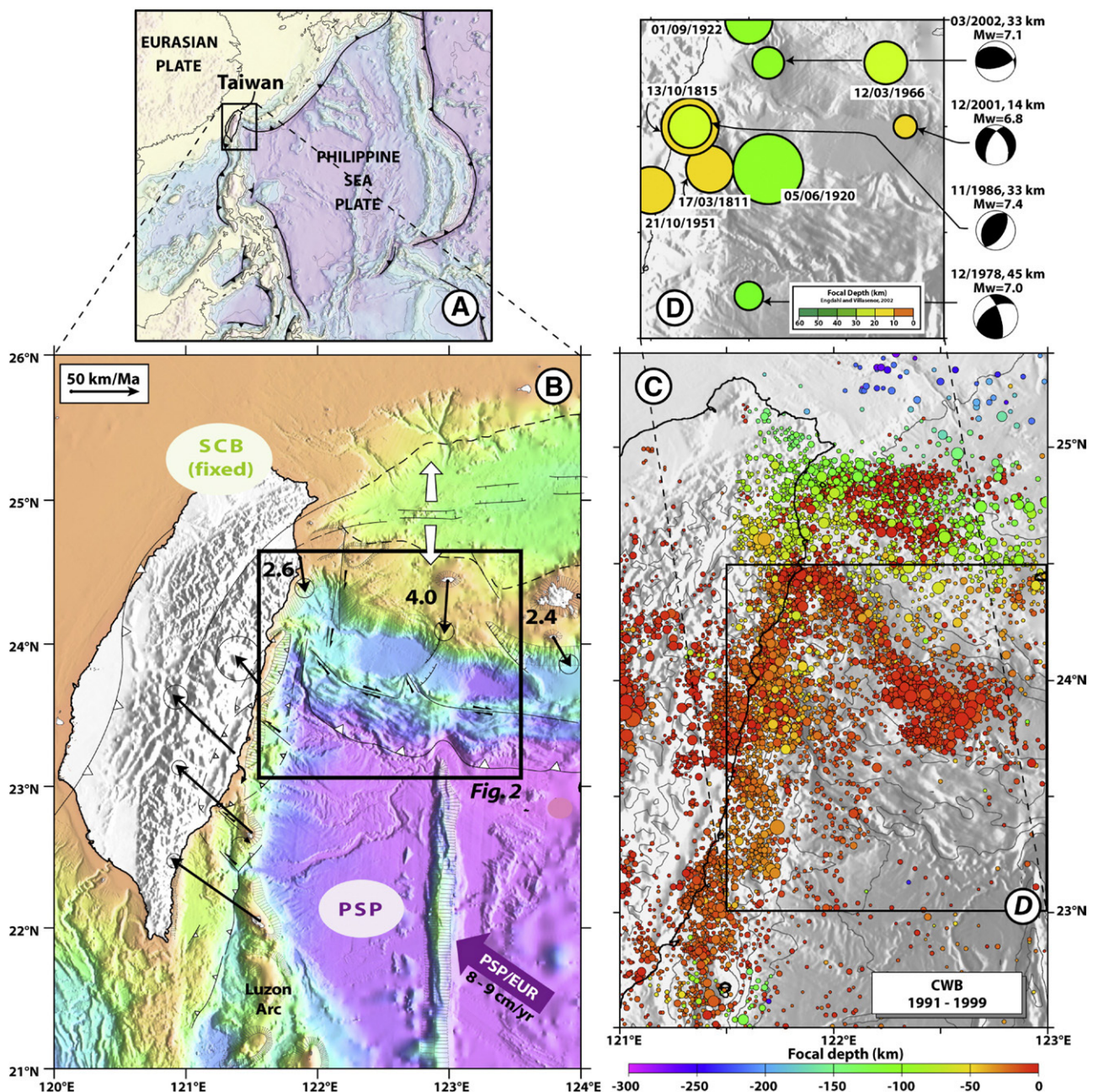


Fig. 1. A. Plate boundaries around Taiwan. B. Geodynamic context of Taiwan (modified after Lallemand and Liu, 1998). C. Seismicity map from 1991 to 1999 (hypocenter catalog from Central Weather Bureau). D. Instrumental seismicity of magnitude earthquake bigger than 7 (from Engdahl and Villasenor, 2002) and studied focal mechanism (see also Table 1).

Table 1  
Earthquakes of magnitude bigger than 7.5 since 1700 and bigger than 7.0 since 2000 occurring offshore eastern Taiwan

Time (year/month/day)	Latitude	Longitude	Depth	Magnitude	Reference
1811/03/17	23.8°N	121.8°E		7.5 (based on intensity)	Tsai (1985)
1815/10/13	24.0°N	121.7°E		7.7 (based on intensity)	Tsai (1985)
1920/06/05	24.0°N	122.0°E		8.1 (Ms)	Wang and Kuo (1995)
			20	8.0 to 8.3 (ML)	IES web site
	23.8°N	122.1°E	35	7.9 (Mw)	Engdahl et al. (1998)
1922/09/01	24.5°N	122.0°E	35	7.5 (Mw)	Engdahl et al. (1998)
1951/10/21	23.7°N	121.5°E	0	7.5 (Mw)	Engdahl et al. (1998)
1966/03/12	24.1°N	122.6°E	63	7.9 (Ms)	Wang and Kuo (1995)
	24.3°N	122.7°E	29	7.4 (Mw)	Engdahl et al. (1998)
			27	7.6 (Ms)	Engdahl and Villasenor (2002)
1978/12/23	23.2°N	122.0°E	45	7.2 (Ms) 7.0 (Mw)	Engdahl and Villasenor (2002)
		122.6°E	21	7.0 (Ms) 7.0 (Mw)	CMT Harvard
1986/11/14	23.9°N	121.6°E	34	7.8 (Ms)	Wang and Kuo (1995)
	24.0°N	121.7°E	28	7.4 (Mw)	Engdahl et al. (1998)
			34	7.7 (Ms)	Engdahl and Villasenor (2002)
	24.0°N	121.8°E	33	7.8 (Ms)	CMT Harvard
2001/12/18	24.0°N	122.7°E	14	7.3 (Ms)	CMT Harvard
		122.8°E	14	6.3 (Ms) 6.8 (Mw) 7.2 (mb)	Engdahl and Villasenor (2002)
2002/03/31	24.3°N	122.1°E	34	7.1 (Mw) 7.2 (mb)	Engdahl and Villasenor (2002)
		122.2°E	33	7.4 (Ms)	CMT Harvard

References are indicated in the table.

Imanishi et al., 1996; Lallemand and Liu, 1998). As a consequence, the relative convergence rate increases across the southernmost Ryukyu Trench and reaches  $\sim 10\text{--}11$  cm/year.

### 3. Review on the Ryukyu subduction structures from previous works

#### 3.1. Ryukyu–Taiwan junction

West of  $123^\circ\text{E}$ , less than 200 km from the Taiwanese collision zone, the E–W trend of the Ryukyu subduction system turns northward, reaching a NW–SE azimuth at its southwestern extremity. East of Taiwan, the southernmost extremity of the Ryukyu Trench was mapped in 1996 using swath bathymetry (Lallemand et al., 1997a; Liu et al., 1998). The Ryukyu deformation front can be clearly followed until  $122^\circ\text{E}$  (Figs. 1 and 2) with the onland suture zone (marked by the Longitudinal Valley Fault, e.g., Angelier et al., 1997) is unclear and the modalities of this transition are still controversial (e.g., Angelier et al., 1990; Hsu and Sibuet, 1995; Chemenda et al., 1995; 1997; Lallemand et al., 1997a,b; Sibuet and Hsu, 1997; Teng et al., 2000; Lallemand et al., 2001).

#### 3.2. Deep part of the subducting PSP ( $>40$ km depth)

The PSP slab, near Taiwan, plunges more steeply than east of the Gagua Ridge and the subducting oceanic crust is estimated to be Early Cretaceous in age, from gabbro dating of the Huatung basin (Deschamps et al., 2000). From seismicity observation, the northward dipping PSP slab is observed down to 300 km depth (Kao, 1998; Font et al., 1999). Tomographic image agrees with seismicity that the southwesternmost extremity of the slab reaches about 120 km depth under northern Taiwan (Rau and Wu, 1995; Wu et al., 1997). Near the slab termination, the slab (between 40 and 120 km) becomes shallower and folded (Font et al., 1999). From recent seismological investigation, Chou et al. (2006) confirm the

slab deformation near Taiwan (between 50 and 100 km depth). The slab deformation, as proposed by Kao (1998), could result from horizontal E–W compression related to the collision between the subducting slab and the root of the Eurasian lithosphere.

#### 3.3. Shallow part of the subducting PSP ( $<40$ km depth)

Based on OBS–MCS refraction performed along 2 arc-parallel lines (Table 2, Line EW-14 and EW-16), many authors (Wang and Chiang, 1998; McIntosh and Nakamura, 1998; Hetland and Wu, 2001; Wang et al., 2004; McIntosh et al., 2005) have shown that the PSP, at latitudes ranging from the accretionary prism to the Ryukyu Arc, also presents high-and-lows geometry. Near Taiwan, the subducting crust presents 2 rises which location is not well determined as it differs regarding the refraction modeling (McIntosh and Nakamura, 1998; Wang et al., 2004). The eastern rise is basically located along the northward prolongation of the Gagua Ridge. The western rise location varies, regarding authors, between the western extremity of the Nanao Basin and the Hoping Basin. Along line EW-14 (McIntosh and Nakamura, 1998; Wang et al., 2004), both rises have an elevation of about 4 km compared to surroundings and, in average, the interplate contact zone is between 15 and 18 km in depth (McIntosh and Nakamura, 1998 or Wang et al., 2004). Wang et al. (2004) interpreted this high-and-low configuration as the buckling of the subducted slab due to increasing lateral compression. Font et al. (2001) proposed that it might correspond to the subduction of an oceanic relief.

#### 3.4. Overriding active margin: Ryukyu Arc basement and forearc sedimentary basins

The analysis of 45 seismic reflection profiles, acquired across the westernmost Ryukyu forearc region, has allowed Font et al. (2001) to map the Ryukyu Arc basement. Beneath the forearc

basins, the Ryukyu basement also displays a high-and-low morphology. The two major basement highs are the Nanao and Hoping Basement Rises (Fig. 2A). Both are flat-top rises about

2 km higher than the neighboring depression. The Nanao Basement Rise is located along the northward prolongation of the Gagua Ridge. The Hoping Basement Rise stands at about 122.2°E. Both Ryukyu basement rises stand above the rises observed in the subducting PSP. Seaward, the Ryukyu basement arc terminates at the northern rear of the accretionary prism, against a set of transcurrent faults (Fig. 2B and C, Font et al., 2001).

Both the Nanao and Hoping Basement rises generated highs on the bathymetry surface, called the Nanao Rise and the Hoping Rise. Those rises delimit the 3 forearc basins (Fig. 2B and C), shallowing westward (Lallemand et al., 1997b; Font et al., 2001). From east to west, they are the East Nanao Basin, the Nanao Basin and the Hoping Basin. The older and highly deformed Suao Basin underlies the Hoping Basin and lies on top of the Hoping Basement Rise. In this study, we focus specifically on the Hopping–Nanao area. Based on bathymetry (see Lallemand et al., 1997b), the Hopping Rise marks a 600-to-700 m elevated surface between the forearc basins. The Hopping Basin is connected to the Nanao Basin by the Hopping Canyon that deeply incises the sedimentary cover of the Hopping Rise (Fig. 2C and B). At this location, based on multichannel seismic reflection lines across the Hopping Rise, the Ryukyu Arc basement is buried beneath 1000 to 2000 m of deformed sediments (Hopping and Suao basins — Figs. 3 and 4).

### 3.5. Mapped near surface faults

In the studied region, from bathymetry and seismic reflection analyses, several modes of deformation affect the forearc structures.

First, the forearc region is dissected by major crustal strike-slip faults (see Figs. 1 and 2). Those faults accommodate the obliquity of the convergence, in a hand, and the rifting of the southern Okinawa trough, in the other hand. Indeed, the convergence obliquity between the PSP and the Ryukyu Arc increases near Taiwan from 40°, east of 123°E, to 60°, west of 122.75°E (Lallemand and Liu, 1998). As a partitioning result, an aseismic trench-parallel transcurrent fault zone is observed along the rear of the Ryukyu accretionary wedge, allowing the southern part of the wedge to be dragged laterally toward Taiwan (Fig. 2B, Dominguez et al., 1998). On seismic profiles, the seaward termination of the Ryukyu basement is obscured by diffractions that are caused by this transcurrent faulting. Since the Ryukyu basement is never recognized seaward of this obscured area, Font et al. (2001) suggested that transcurrent faults developed at the seaward termination of the basement. The transcurrent fault zone would therefore develop within the sedimentary prism. The opening of the southern Okinawa Trough has been quantified by GPS, evidencing the differential motion between the Ilan Plain and the Yonaguni Island (123°E — Fig. 1B). To accommodate the differential motion

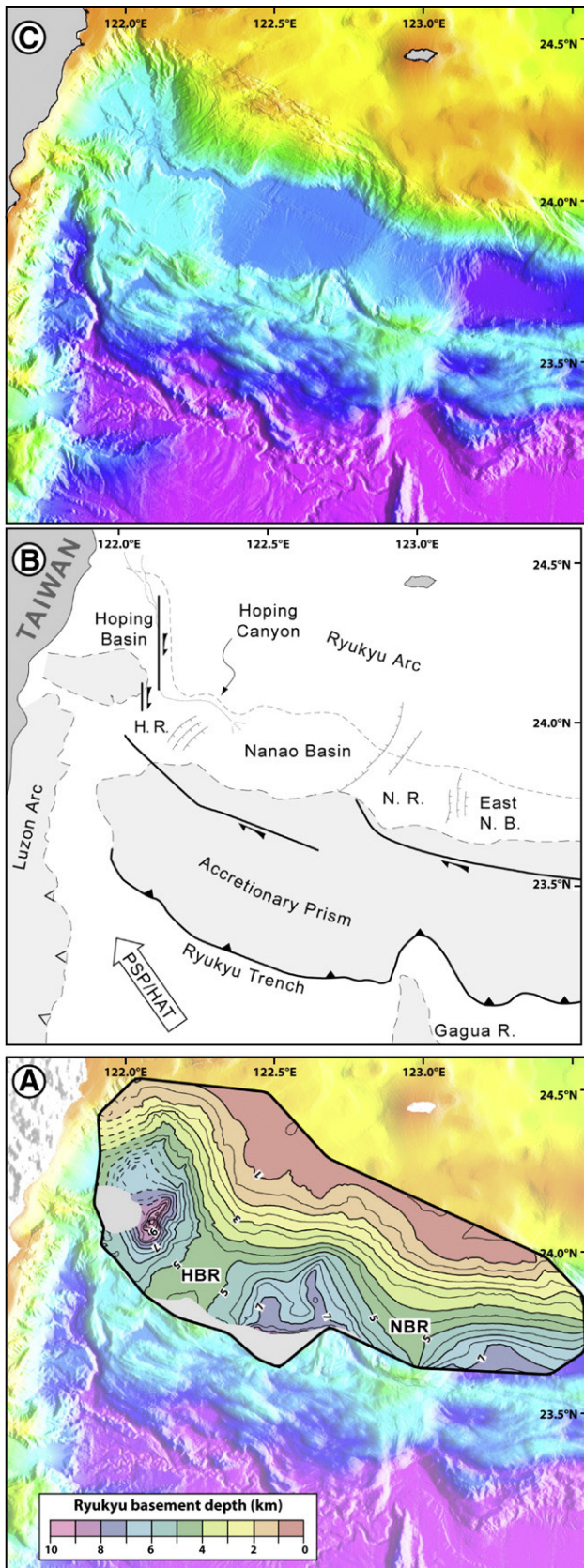


Fig. 2. A. Ryukyu basement map below sea-level (sedimentary cover has been removed, Font et al., 2001). HBR = Hopping Basement Rise; NBR = Nanao Basement Rise. B. Regional geodynamic context of the southernmost Ryukyu subduction system (modified after Font et al., 2001). H.R. = Hopping Rise; N.R. = Nanao Rise; East N. B. = East Nanao Basin. C. Detailed bathymetry map of the same area.

Table 2

List and location of published multichannel and refraction seismics in the southernmost Ryukyu forearc region

**MCS lines published across the Hopping Rise**

MCS 367-07

Lallemand et al. (1997)

ACT 65

Lallemand et al. (1999)

EW 14; 446-5; 446-11

Font et al. (2001)

EW 14

Schnurle et al. (1997)

**Refraction lines published across the Hopping Rise**

EW 14; EW 16

Hetland and Wu (2001);

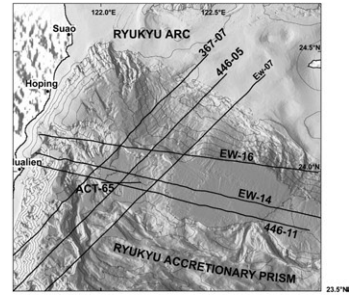
McIntosh and Nakamura (1998);

Wang and Chiang (1998);

Wang et al. (2004)

EW 16

McIntosh et al. (2005)



between the two blocks, Lallemand and Liu (1998) have proposed a N–S transform fault zone cutting through Ryukyu Arc from the Southern Okinawa Trough to the accretionary prism (Fig. 2B). This fault zone offsets clockwise the Ryukyu Arc, causing a bayonet-shape in the arc slope. A flower structure in the

Hopping and Suao sedimentary basins evidenced this N–S transform fault on several seismic profiles (e.g. Figs. 3 and 4).

A second mode of deformation affects the Ryukyu Arc basement. NNE–SSW normal faults are observed on the flanks of both Ryukyu basement highs, offsetting the top of the

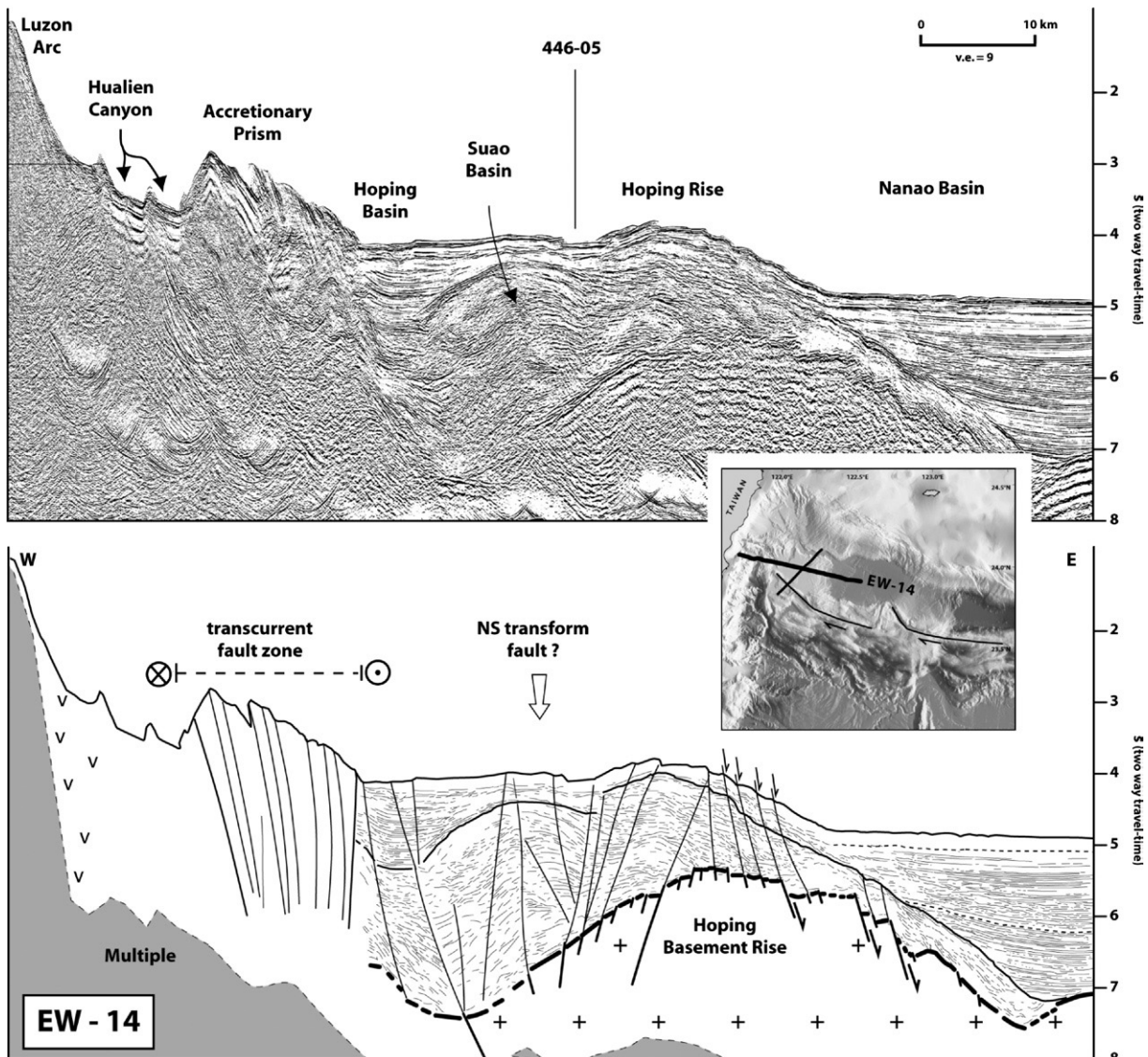


Fig. 3. Section of seismic profile EW-14 (after Font et al., 2001).

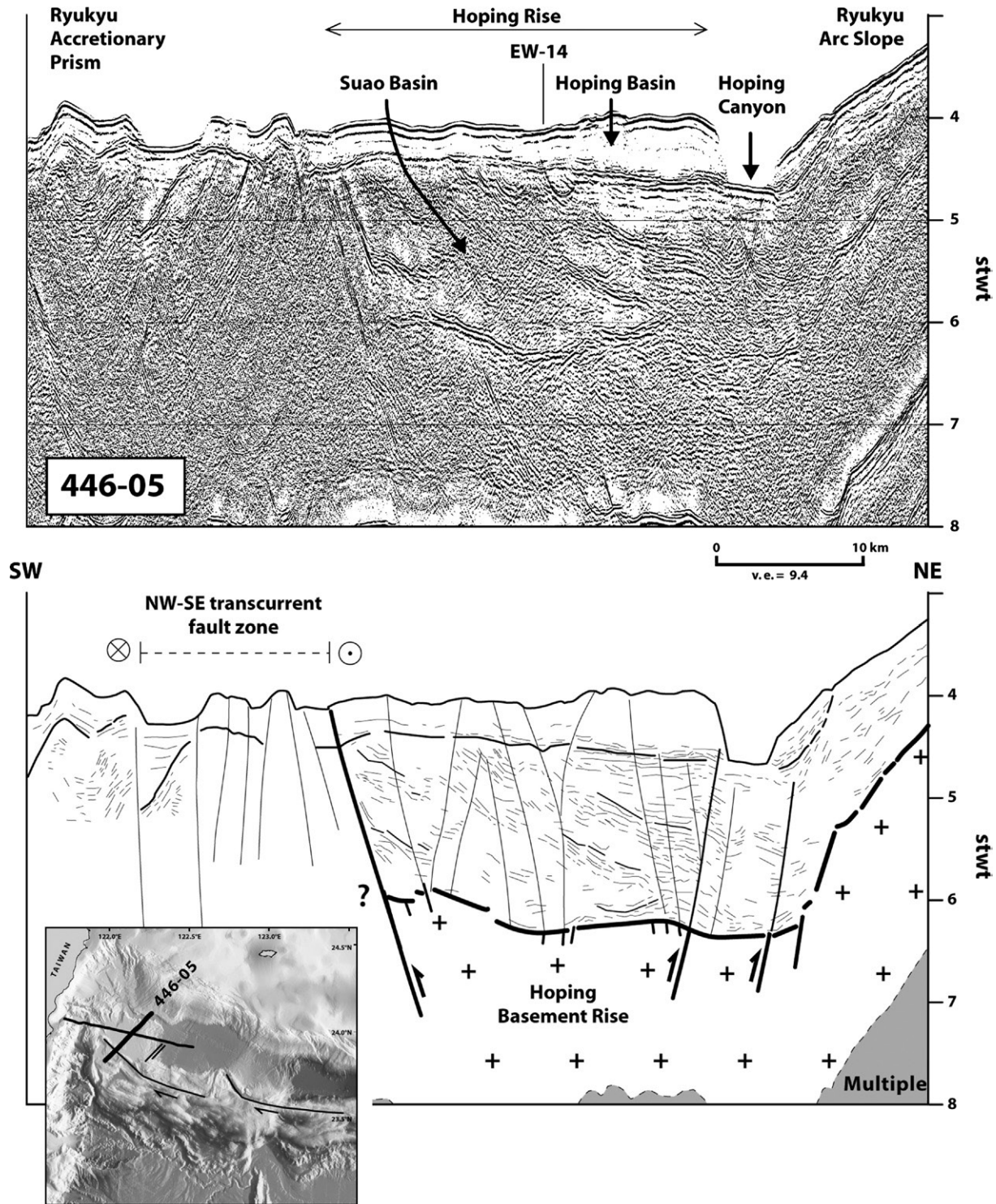


Fig. 4. Section of seismic profile ORI 446-05 (modified after Font et al., 2001).

basement and cutting through the entire sedimentary sequence (e.g. Fig. 3). This configuration evidences that portions of the arc basement are presently rising. The Nanao Basement Rise uplift has been related with the oblique subduction of the Gagua Ridge (Schnurle et al., 1998) and is still going on. The Hoping Basement Rise presents the same deformation characteristics than the Nanao Basement Rise on its eastern flank (the western

one being affected by the N–S transform fault — Fig. 3). The most recent sediment on top of the rise are also affected by normal fault, indicating that the Hoping Basement is also still active. Font et al. (2001) proposed that the uplift process is generated by the subduction (or underplating) of some local oceanic relief. The nature of this topographic asperity could either be a detached block of the Luzon Arc (in agreement with

geodynamic reconstruction of Malavieille et al., 2002), an isolated seamount or some material removed from the frontal part (southernmost extremity) of the Ryukyu margin.

A third mode of deformation is illustrated on the seismic line ORI-446-5 (Fig. 4). A set of high-angle faults cut through the Hoping Rise, showing an apparent reverse offset. The Hoping canyon, that deeply incises the sedimentary cover as the Hoping Basement rises up, seems controlled by one of them. At this location, the Ryukyu Arc basement top presents an 800 m-high vertical offset just beneath the Hoping canyon. This fault perfectly aligns with the Hoping Canyon. Note that the fault, which apparently normally offsets the Ryukyu Basement at the southern base of the Ryukyu Arc slope, is no longer visible to the east and to the west of the Hoping Canyon (see, for example, Line EW-01, Schnurle et al., 1998). Because, we clearly observed trench-parallel active extension (see above), we favor the interpretation of these high-angle faults – trending perpendicular to the normal faults – as reverse faults delimiting a pop-up structure in a global trench-perpendicular compressional environment. We cannot exclude strike-slip component along these steeply dipping faults. Furthermore, regarding recent geodynamic reconstruction (Lallemand et al., 2001), this region was, a few million years ago, located on an ocean–continent boundary. This position could explain the apparent normal offset of a fault set that would be now undergoing compression.

#### 4. Earthquake distribution based on new hypocentral dataset

In the Ryukyu subduction southernmost extremity, summarizing briefly what is said above, seismic refraction modeling shows a disturbed interplate contact zone (with highs-and-lows geometry) and seismic reflection analyses evidences that the Ryukyu basement is affected by all modes of faulting and deformation. Seismicity in the offshore area corresponds to several dense earthquake clusters (Kao, 1998; Font et al., 1999; Kao et al., 2000): over the Southern Okinawa back-arc Trough, in the forearc region, near the plate interface and along the Coastal Range — Luzon Arc (Fig. 1C).

In this paper, we focus on the densest seismic cluster located near the Hoping Rise, in the forearc region, where several major earthquakes occurred in the past. We aim to assess the fault geometries revealed by earthquake distribution and their tectonic significance in relation with recognized structures of the area. Because of the nearby population, we wish to draw attention on the risk potentiality of those faults. However, in this offshore area, earthquake location determined by the Central Weather Bureau of Taiwan shows large location uncertainties. In the following section, we illustrate the earthquake distribution using a refine seismological dataset from Font et al. (2004). Prior to discuss this distribution, we synthesize very succinctly the earthquake location process. The reader should refer to Font et al. (2004) for more detailed information on this topic.

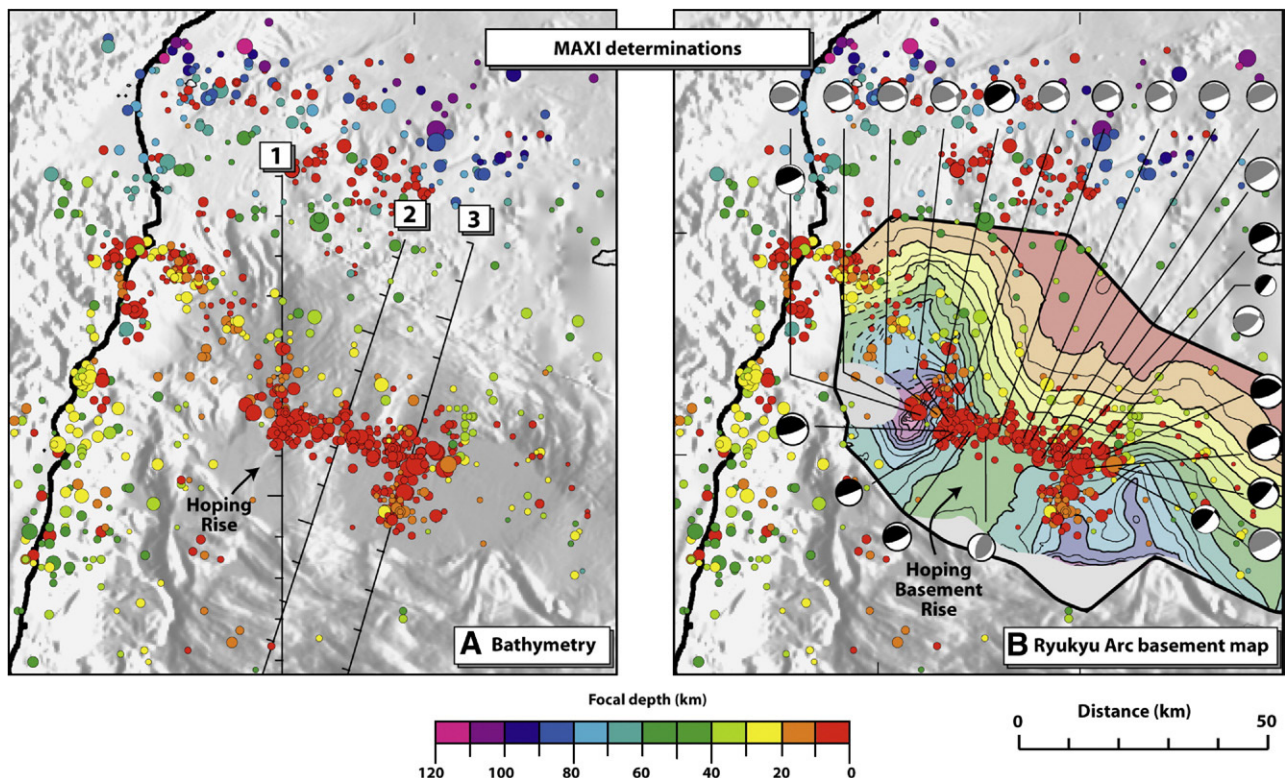


Fig. 5. 3D hypocenter determinations from Font et al. (2004). A. Seismicity on the bathymetry. Note that earthquakes are well aligned with the Hoping Canyon. Cross-sections location corresponds to Fig. 7. B. Seismicity and focal mechanisms (grey beach-balls are from Kao, 1998, black ones are from Harvard CMT catalog, Dziewonski et al., 1988) on top of the Ryukyu basement map. Note that seismicity perfectly surrounds the Hoping Rise and Hoping Basement Rise.

#### 4.1. Data and method

Font et al. (2004) apply the Maximum Intersection method (MAXI), to the absolute location of local earthquakes occurring offshore eastern Taiwan. This method is well adapted for investigations based on local seismic data and subduction zone because it allows the use of 3D velocity models presenting strong lateral heterogeneities. In the following section, we summarize the MAXI method, the 3D velocity model construction (Font et al., 2003) and the data used to obtain the refine hypocenter dataset.

##### 4.1.1. Method

The MAXI method determines, within a 3D velocity model, the absolute location of each earthquake independently based on measurements of arrival times. The algorithm used for this study is fundamentally different from classical determination method because it is based on the concept of Equal Difference Time surfaces (EDT surfaces — Zhou, 1994) that are established from P-wave measurement differences at pairs of stations. Basically, the method can be summarized into 3 steps. First, the algorithm seeks for the spatial node of the velocity model that is crossed by the maximum number of EDT surfaces, i.e., the spatial node that better satisfies the arrival time differences computed at all station

pairs. This node is called PRED, standing for predetermination solution. The great advantage of this search mode is that it depends neither on the origin time estimate nor on any residual minimization. Second, thanks to the PRED characteristics, residual outliers can be objectively detected and are cleaned out from the original dataset, without any iterative process or weighting. Then, in a third step, a statistical minimization is conducted in a small domain around the PRED node, which results in a unique FINAL solution. The MAXI method is applied in the southernmost extremity of the Ryukyu subduction zone with the proper station correction terms. This static term at each station (e.g. Font et al., 2004) rectifies systematic errors, such as different clocks between the 2 networks used (see Chou et al., 2006) and/or velocity anomalies beneath the station.

##### 4.1.2. Velocity model

Due to the inhomogeneous station coverage of the local seismic networks, there is no detailed tomographic study offshore eastern Taiwan. Accordingly, Font et al. (2003) has integrated all geophysical data in order to built a 3D comprehensive velocity model in the offshore domain based on seismic reflection and refraction profiles, Earth model iasp91 (Kennett and Engdahl, 1991) and global seismicity (Engdahl et al., 1998). The offshore model is then combined with an onland tomographic model (Rau

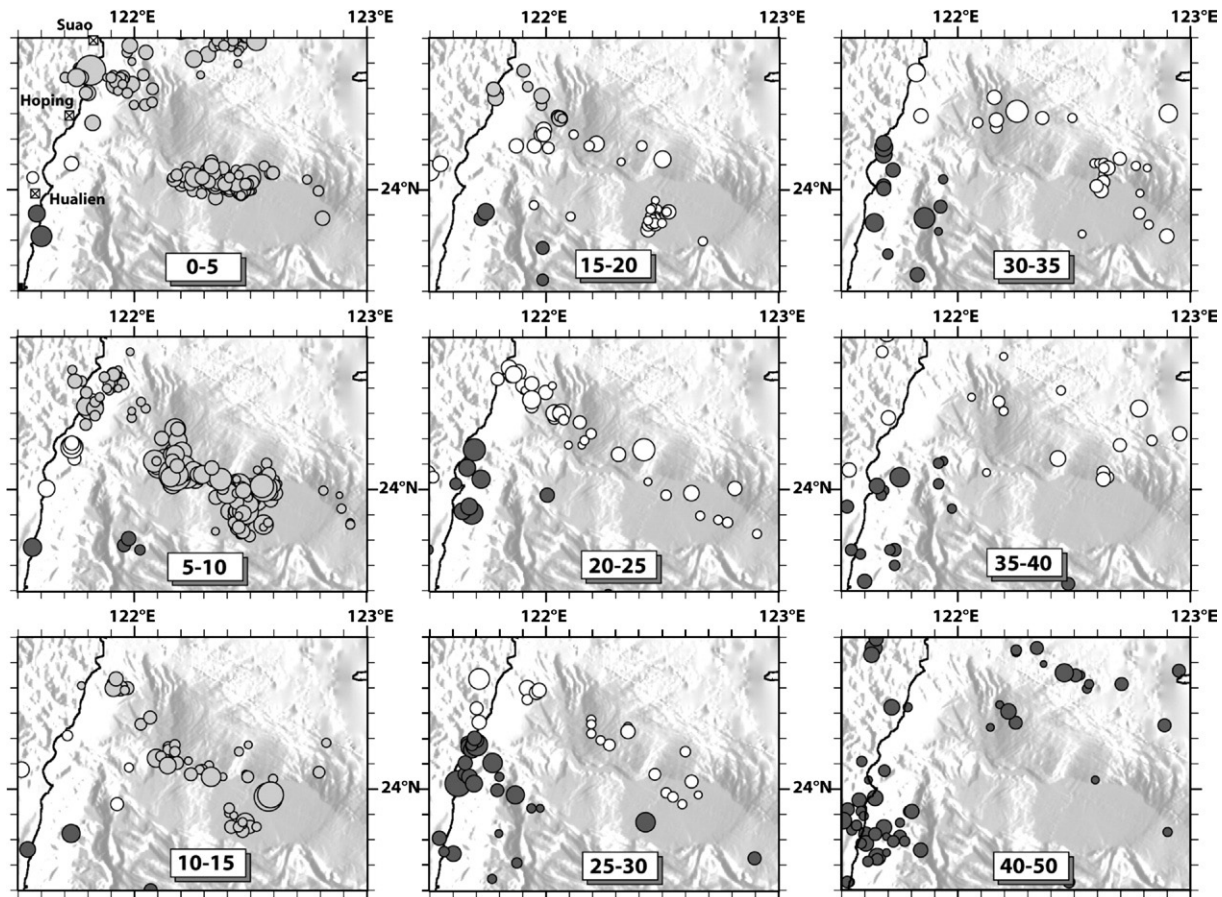


Fig. 6. Horizontal cross-section of the 3D hypocenter determinations. Thickness and depth of each cross-section are indicated on the figure. Light grey seismicity occurs in the overriding Ryukyu Arc; dark grey seismicity occurs within the Philippine Sea Plate. White seismicity is on the Seismogenic Plate Interface or indeterminate.

and Wu, 1995) to create the first comprehensive 3D Vp model for the region (Font, 2001; Font et al., 2003).

#### 4.1.3. Seismic data

Font et al. (2004) improved the offshore earthquake azimuthal coverage by combining the data from the two independent networks that surround the study area: the Central Weather Bureau from Taiwan and the Japanese Meteorological Agency seismic networks. Authors selected all seismic stations distributed in the velocity model with an elevation lower than 2 km and that continuously recorded from 1992 to 1997. Their set of seismic stations was composed of 29 Taiwanese stations distributed along the eastern coast between northern Taiwan and Lanyu Island, and 4 Japanese stations located on the closest Japanese islands. All selected earthquakes have been recorded by at least 7 of the Taiwanese stations (with a very good to good quality estimate) and at least 3 of the 4 Japanese stations. Between 1992 and 1997, they obtained 1139 seismic events common to both seismic networks, with a minimum of 10 P-arrivals records by earthquake, for a total of 28,514 P-arrival times.

#### 4.1.4. Hypocentral location uncertainties

Font et al. (2004) demonstrates that classical hypocentral determination as well as location uncertainties purely corresponds to mathematical solution and do not represents a real value. However, it is commonly expected in hypocentral determination investigation to give an evaluation of the error parameter. The estimate of errors is based on arrival time residues evaluated for the spatial location of the final hypocenter, in the 3D velocity model (Font et al., 2003). In average, location error is of 3.7 km (with a standard deviation of 1.9 km).

## 4.2. Results

The location of earthquakes, recorded at both the Taiwanese and Japanese networks, is achieved for 1117 events (Fig. 5 — results presenting a quality parameter lower than 0.6 have been removed, Font et al., 2004). In this paper, we focus our interest on the cluster located in the Hopping–Nanao forearc area (between 122.1°E–122.5°E and 23.5°N–24.5°N).

#### 4.2.1. Distribution of seismic structures

To describe earthquake spatial distribution, we distinguish shallow earthquakes occurring within the overriding margin from deeper ones nucleating near the plate interface. This distinction is based on wide-angle/refraction data that helped to image the plate interface down to ~30 km (e.g. Wang and Chiang, 1998; McIntosh and Nakamura, 1998). Deeper seismic events occurring within the subducting plate will not be discussed in this paper.

**4.2.1.1. Ryukyu margin earthquakes.** Seismic events in the forearc area are mainly distributed within the overriding Ryukyu Arc, in a shallow domain down to 20 km in depth (Figs. 6 and 7). Earthquakes that cut through the Ryukyu Arc distribute along three main trends. A 40 km-long N110°-trending seismic structure, the densest seismic cluster over the whole eastern Taiwan, aligns along the Hopping Canyon (Figs. 5

and 6). We call this N110°-cluster the Hopping Canyon (HC) cluster. The HC cluster is bounded, to the west and to the east, by two minor N–S-trending seismic segments.

The N–S segment located west of the HC cluster extends between 5 and 12 km depth and parallels a N–S offset of the Ryukyu Arc observed in the bathymetry. Section 1 (Figs. 7 and 5) through this segment shows that earthquakes are distributed in the overriding Ryukyu margin along a plane that dips ~20–30° northward.

Most of the earthquakes constituting the HC cluster occur between 5 and 10 km depth (including 3 earthquakes of magnitude mb bigger than 6.0). The cluster direction strikes N110° from sea-bottom down to 12 km depth. At depths greater than 15 km, the earthquakes (white dots on Fig. 6) occur near the plate interface and thus do not belong to the same cluster. No specific dip can be deduced from shallow events on section 2

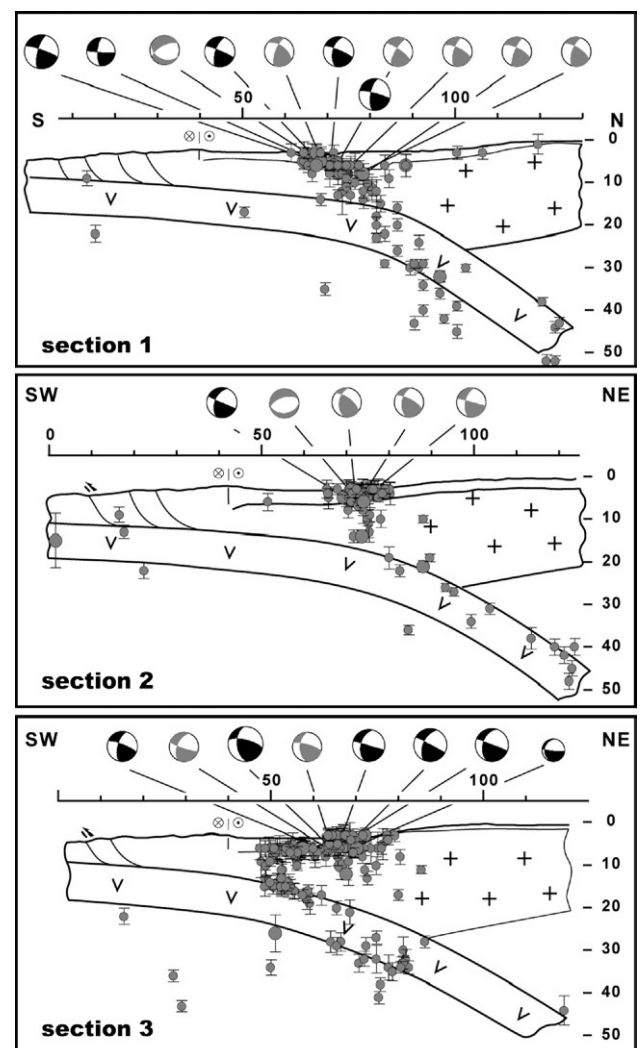


Fig. 7. Cross-sections in the 3D hypocenter determinations (location map is presented on Fig. 5). See Fig. 5 for focal mechanism references. Note that for each section, the top of the Ryukyu Arc is constrained from multichannel seismic reflection analysis (Font et al., 2001) and that the top of the Philippine Sea Plate is drawn from seismic reflection, wide-angle seismic data and global and local seismicity (see Font, 2001).

(Fig. 7). The projection of the relocated earthquakes on wide-angle modeling (Fig. 8) confirms that this cluster occurs within the Ryukyu margin.

The N–S segment located east of the HC cluster is essentially superficial between 5 and ~10 km depth (Fig. 6). Again, no specific dip can be deduced from section 3 (Fig. 7).

**4.2.1.2. Subduction interface events.** A group of events at depths between 12 and 22 km beneath the eastern Hoping Rise on section 3 (Fig. 7) perfectly align along the subduction interface. Those earthquakes also well align along the subduction interface when projected on wide-angle profile EW-01 (Fig. 8).

Some events also align along the expected subduction plane on section 1 (between 15 and 20 km depth) and 2 (between 20 and 50 km depth), not beneath the forearc basins but only beneath the slope of the arc, i.e., northward.

#### 4.2.2. Focal mechanisms

Two datasets from Kao (1998) and from Harvard catalog (Dziwonski et al., 1981) of focal mechanisms are used in this study. In order to be consistent with the 3D hypocentral determinations, we have selected all focal mechanisms within the Hoping Cluster that happened between 1992 and 1997 and that matched with relocated hypocenters. Totally 24 events

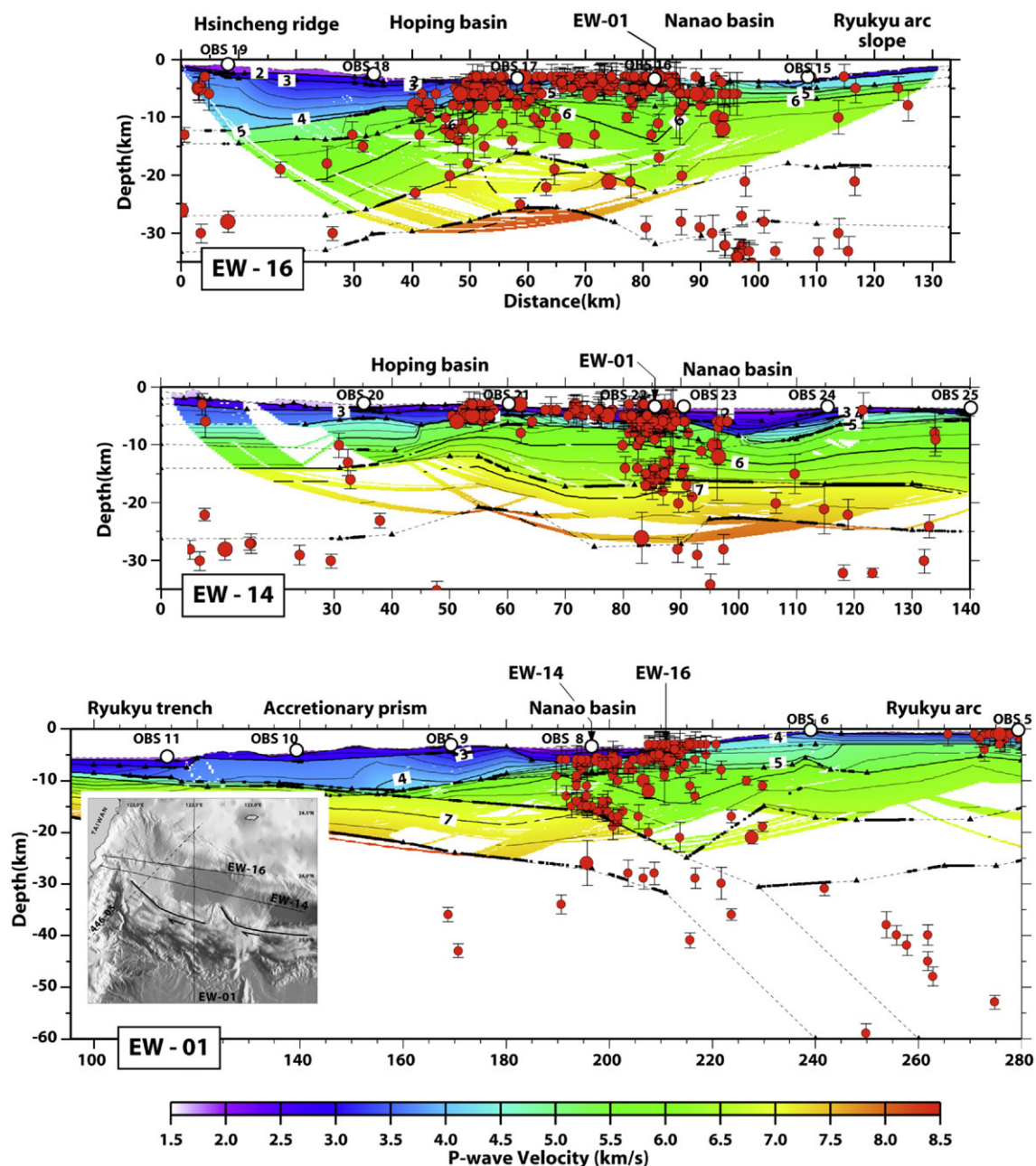


Fig. 8. Seismicity cross-section superimposed to TAICRUST refraction modeling from Wang et al., 2004. Each seismicity cross-section is 20 km thick.

correspond to our data selection. All focal mechanisms are coherent, identifying a thrust fault associated with the shallow earthquake cluster aligning with the Hopping Canyon. The averaged nodal plane is either 25° northward dipping N110°-striking thrust, or 75° high-angle N75° reverse fault.

## 5. Discussion

From the above description, we observe that the cluster of earthquakes below the forearc area is composed of two groups. The largest is extremely shallow, especially in the middle part of the swarm. A second group of quakes distributes deeper near the plates interface. This second group is visible mainly on sections 1 and 3 (Fig. 7), i.e., at both ends of the cluster. The main segment of the cluster coincides with the Hopping Canyon, which is known to be structurally controlled (Font et al., 2001), and most quakes wrap the slope break in the arc's basement between the Ryukyu Arc slope and the flat-top Hopping Basement Rise.

We consider that the deeper group corresponds to subduction earthquakes — since it clusters in the vicinity of the expected subduction plane, and is undoubtedly distinct from the shallow one. The subduction plate interface is well imaged in the area. The *décollement* can be traced below the accretionary wedge 10 km arcward of the trench (Line 367-9 in Lallemand et al., 1997b). Northward, the top of the subducting Philippine Sea plate is constrained by seismic refraction profiles (McIntosh and Nakamura, 1998; Wang and Chiang, 1998; Wang et al., 2004) and seismicity (Kao, 1998). Based on this 6-year seismological dataset, we can say that the updip limit of the seismogenic zone is about – and no deeper than – 12 km (i.e., depth on the 3 sections, Fig. 7). The reason for such a shallow depth below the Hopping Rise on sections 1 and 3 (or on EW-01, Fig. 8) compared to a deeper one below the arc slope (on section 2), is certainly related to the slab geometry — shallower beneath the Hopping Rise.

Focusing on the shallow group, we envisage 2 different scenarios to interpret the seismicity (Fig. 9). To constrain our

arguments, we use focal mechanism data (Dziewonski et al., 1988; Kao, 1998)

- Scenario 1: Shallow 25°-dipping N110°-striking thrust cutting through the cluster and emerging on the seafloor in the middle part of the Hopping Rise.
- Scenario 2: 75° high-angle N75°-striking reverse fault cutting through the cluster and emerging in the Hopping Canyon.

### 5.1. Seismicity and focal mechanisms

Both dip and strike of focal mechanism nodal planes are extremely homogeneous. Looking at the distribution of epicenters, especially along the main branch of the cluster, we can observe that the 25°-dipping N110°-striking thrust issued from focal mechanism data (Fig. 9, scenario 1) is the only one which directly fits with the N110°-trending HC cluster. On the counter part, one may take into account the narrowness of the main branch to support a high-angle reverse back-thrust instead of a shallow-dipping one. In this case, we would need to consider a spatial organization with short *en-échélon* N75° back-thrusts to fit the nodal plane azimuth to the seismicity distribution (Fig. 9, scenario 2).

### 5.2. Additional constraints: bathymetry and seismic reflection data

This area was intensively surveyed during the last 15 years and we can confront both our scenarios to additional forearc observations such as seafloor morphology or seismic structure summarized in the first part of this paper (see Table 2 for references to published seismic lines).

The main result we conclude from the analysis of the seismic lines is that present-day surface expression of active faulting reveals trench-parallel extension and trench-perpendicular compression in the region of the Hopping Rise. This stress

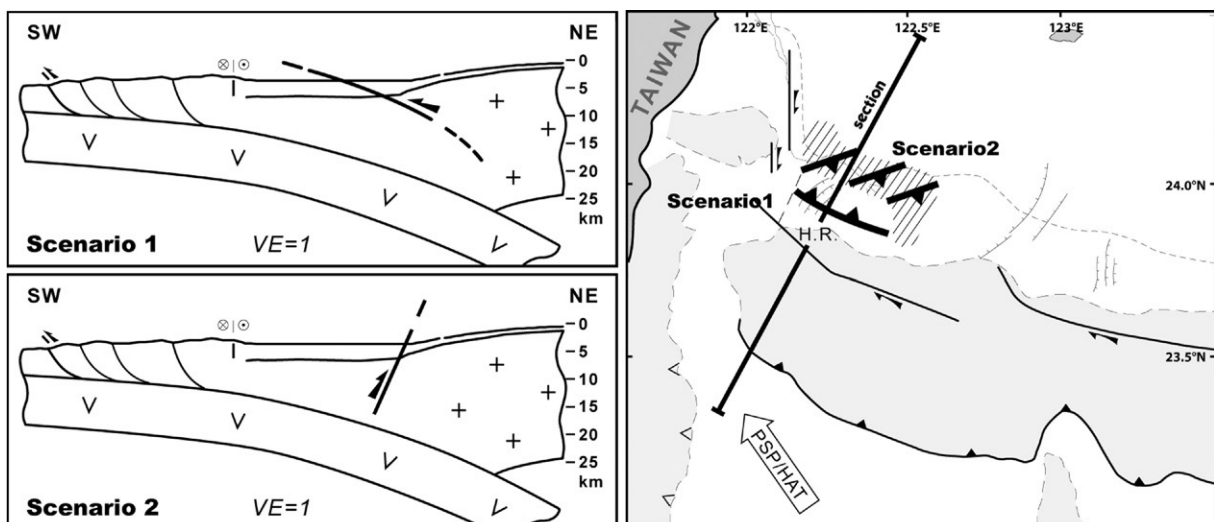


Fig. 9. Schematization of the 2 scenarios proposed in the text on cross-section (left panel) and on map (right panel). We conclude that the scenario (2) is the most plausible. H.R. = Hopping Rise. Hs.R. = Hsincheng Ridge.

regime most certainly illustrates extrados faulting accompanying the uplift of the HBR which is itself accommodated by high-angle reverse faulting. Both types of active faulting better agree with the scenario 2 that supposes high-angle faulting.

Scenario 1 will result in a subsidence of the “Hoping Rise region” rather than an uplift because it would be overthrust by the Ryukyu Arc slope. Furthermore, there is no evidence of shallow-dipping forward thrust emergence in the southern area of the Hoping Rise as we would expect based on hypocenters locations.

### 5.3. Additional constrains: refraction data

Based on OBS–MCS refraction performed along 2 arc-parallel lines, many authors (Wang and Chiang, 1998; McIntosh and Nakamura, 1998; Hetland and Wu, 2001; Wang et al., 2004; McIntosh et al., 2005) have shown that the Hoping Rise coincided with a shallower plate interface, i.e. ~5 km shallower compared to its lateral position on each side of the Hoping Rise. To explain this shallow interface, Wang et al. (2004) suggest a “buckling” of the subducted Philippine Sea plate. The extremely short wavelength of this buckling is hard to explain if we consider that the subducting oceanic crust is as old as Early Cretaceous (Deschamps et al., 2000), but other heterogeneities can be invoked such as intraplate thrusting (comparable to the Zenisu Ridge near Japan, Chamot-Rooke and Le Pichon, 1989). In any case, the velocity structure supports the hypothesis of a subducting oceanic relief. In other words, we expect that a rise in the subducting plate generates a rise of the subduction interface and in the above margin.

## 6. Conclusion

This study precisely images the earthquake distribution in the forearc cluster occurring offshore eastern Taiwan. Absolute hypocenter locations have been determined using the 3D MAXI location process. Font et al. (2004) conducted this procedure within a 3D velocity model by combining the Taiwanese and neighboring Japanese networks. Six years of data (~1100 events) commonly recorded at both networks are presented in this work.

Earthquakes distribute mainly along 2 active planes. The first one aligns along the subduction plate interface and the second one, shallower, occurs within the overriding margin. All focal mechanisms on the recording period are located in the shallow group and present nodal planes compatible with thrust faults.

By integrating the new seismological image to the regional context, we conclude that an intense seismicity affects the Ryukyu forearc basement along morphostructural features suggesting that the Hoping Rise is structurally controlled by active faults. The seismic deformation (from focal mechanism nodal planes) exclusively indicates reverse faulting revealing that the forearc basement undergoes trench-perpendicular strong compression. Based on additional data, we suspect that the subduction of an oceanic relief causes simultaneously trench-perpendicular compression and trench-parallel extension in the forearc. These tectonic regimes associated with the uplift of the Hoping Rise above the subducting high suggest the existence of a pop-up structure in the Hoping Rise area.

However, this solution does not simply satisfy the strike of the nodal planes since *en-échélon* short faults are required rather than a single 40 km-long thrust that would easier explain the occurrence of magnitude 6, or even 7 earthquakes. To properly image active faults and evaluate seismic risk in this domain located only a few tens of kilometers from Taiwanese Coast, it is necessary to deploy a dense array of ocean bottom seismometers above the seismogenic area.

## Acknowledgements

Jacques Angelier, Nicole Béthoux, Bernard Célrier, Xavier Le Pichon, Jacques Malavieille and Françoise Sage are thanked for their constructive comments on the seismotectonic significance of the study area. Many of the figures are generated using the GMT software of Wessel and Smith. The Ministry of Education, Republic of China kindly provided scholarships to the first author through the office of Bureau de Representation de Taipei en France during her PhD. study in Taiwan. Both the National Science Council and the French Institute in Taiwan support the France–Taiwan cooperation frame in Earth Science. This research was funded by the National Science Council of the Republic of China to C.-S. Liu through grants NSC83-0209-M-002a-031Y, NSC85-2611-M-002-005Y and NSC86-2117-M-002a-001-ODP.

## References

- Angelier, J., Bergerat, F., Chu, H.-T., Lee, T.-Q., 1990. Tectonic analysis and the evolution of a curved collision belt: the Hsuehshan Range, northern Taiwan. *Tectonophysics* 183 (1–4), 77–96.
- Angelier, J., Chu, H.-T., Lee, J.-C., 1997. Shear concentration in a collision zone: kinematics of the Chihshang Fault as revealed by outcrop-scale quantification of active faulting, Longitudinal Valley, eastern Taiwan. *Tectonophysics* 274, 117–143.
- Chamot-Rooke, N., Le Pichon, X., 1989. Zenisu Ridge: a mechanical model of formation. *Tectonophysics* 160, 175–193.
- Chemenda, A.I., Mattauer, M., Bokun, A.N., 1995. A mechanism for syn-collisional deep rock exhumation and associated normal faulting: results from physical modeling. *Earth Planet. Sci. Lett.* 132, 225–232.
- Chemenda, A.I., Yang, R.-K., Hsieh, C.-H., Groholsky, A.L., 1997. Evolutionary model for the Taiwan collision based on physical modelling. *Tectonophysics* 274 (1–3), 253–274.
- Chou, H., Kuo, B., Hung, S., Chiao, L., Zhao, D., Wu, Y., 2006. The Taiwan–Ryukyu subduction–collision complex: folding of a viscoelastic slab and the double seismic zone. *J. Geophys. Res.* 111 (B04410), 1–14. doi:10.1029/2005JB003822.
- Deschamps, A., Monie, P., Lallemand, S., Hsu, S.-K., Yeh, K.Y., 2000. Evidence for Early Cretaceous oceanic crust trapped in the Philippine Sea Plate. *Earth Planet. Sci. Lett.* 179, 503–516.
- Dominguez, S., Lallemand, S., Malavieille, J., Schnurle, P., 1998. Oblique subduction of the Gagua Ridge beneath the Ryukyu accretionary wedge system—insight from marine observations and sandbox experiments. *Mar. Geophys. Res.* 20 (5), 383–402.
- Dziwonski, A.M., Chou, T.-A., Woodhouse, J.H., 1981. Determination of earthquake source parameters from waveform data for studies of global and regional seismicity. *J. Geophys. Res.* 86, 2825–2852.
- Dziwonski, A.M., Ekström, G., Franzen, J.E., Woodhouse, J.H., 1988. Global seismicity of 1982 and 1983: additional centroid-moment tensor solutions for 553 earthquakes. *Phys. Earth Planet. Inter.* 53, 17–45.
- Engdahl, E.R., Villasenor, A., 2002. Global seismicity: 1900–1999. In: Lee, W.H.K., Kanamori, H., Jennings, P.C., Kisslinger, C. (Eds.), *International Handbook of Earthquakes Engineering and Seismology, Part A*, pp. 665–690.

- Engdahl, E.R., Van Der Hilst, R.D., Buland, R., 1998. Global teleseismic earthquake relocation with improved travel times and procedures for depth relocation. *Bull. Seismol. Soc. Am.* 88, 722–743.
- Font, Y., 2001. Modes of the ongoing arc-continent collisional processes in Taiwan: new insights from seismic reflection analyses and earthquake relocation. Ph. D. Thesis, National Taiwan University, Taipei, 262 pp.
- Font, Y., Lallemand, S., Angelier, J., 1999. Etude de la transition entre l'orogène actif de Taiwan et la subduction des Ryukyu-Apports de la sismicité. *Bull. Soc. Geol. Fr.* 170 (3), 271–283.
- Font, Y., Liu, C.-S., Schnurle, P., Lallemand, S., 2001. Constraints on backstop geometry from the southwest Ryukyu subduction based on reflection seismic data. *Tectonophysics* 333, 135–158.
- Font, Y., Kao, H., Liu, C.-S., Chiao, L.-Y., 2003. A comprehensive 3D seismic velocity model for the eastern Taiwan–southernmost Ryukyu regions. *Terr. Atmos. Ocean. Sci.* 14 (2), 159–182.
- Font, Y., Kao, H., Lallemand, S., Liu, C.-S., Chiao, L.-Y., 2004. Hypocentral determination offshore Eastern Taiwan using the Maximum Intersection method. *Geophys. J. Int.* 158 (2), 655–675.
- Hetland, E., Wu, F., 2001. Crustal structure at the intersection of the Ryukyu Trench with the arc-continent collision in Taiwan: results from offshore–onshore seismic experiment. *Terr. Atmos. Ocean. Sci.* 12, 231–248.
- Ho, C.-S., 1986. A synthesis of the geologic evolution of Taiwan. *Tectonophysics* 125, 1–16.
- Hsu, S.K., Sibuet, J.C., 1995. Is Taiwan the result of arc-continent or arc–arc collision? *Earth Planet. Sci. Lett.* 136 (3–4), 315–324.
- Imanishi, M., Kimata, F., Inamori, N., Miyajima, R., Okuda, T., Takai, K., Hiraha, K., 1996. Horizontal displacements by GPS measurements at Okinawa–Sakishima Islands (1994–1995). *Earthquake* 2 (49), 417–421 (in Japanese).
- Kao, H., 1998. Can great earthquakes occur in the southernmost Ryukyu Arc–Taiwan region. *Terr. Atmos. Ocean. Sci.* 9 (3), 487–508.
- Kao, H., Chen, R.-V., Chang, C.-H., 2000. Exactly where does the 1999 Chi-Chi earthquake in Taiwan nucleate? *Terr. Atmos. Ocean. Sci.* 11, 567–580.
- Kennett, B.L.N., Engdahl, E.R., 1991. Travel times for global earthquake location and phase identification. *Geophys. J. Int.* 105, 429–465.
- Lallemand, S., Liu, C.-S., 1998. Geodynamic implications of present-day kinematics in the southern Ryukyus. *J. Geol. Soc. China* 41 (4), 551–564.
- Lallemand, S., Liu, C.-S., Angelier, J., Collot, J.Y., Deffontaines, B., Dominguez, S., Fournier, M., Hsu, S.-K., Le Formal, J.-P., Liu, S.-Y., Lu, C.-Y., Malavieille, J., Schnurle, P., Sibuet, J.-C., Thureau, N., Wang, F., 1997a. Swath bathymetry reveals active arc-continent collision near Taiwan. *EOS* 78 (17), 173–175.
- Lallemand, S., Liu, C.-S., Font, Y., 1997b. A tear fault boundary between the Taiwan orogen and the Ryukyu subduction zone. Special issue of *Tectonophysics on Active Collision in Taiwan* 274 (1–3), 171–190.
- Lallemand, S., Font, Y., Bijwaard, H., Kao, H., 2001. New insights on 3-D plates interaction near Taiwan from tomography and tectonic implications. *Tectonophysics* 335, 229–253.
- Liu, C.-S., Liu, S.-Y., Lallemand, S., Lundberg, N., Reed, D., 1998. Digital elevation model and its tectonic implications. *Terr. Atmos. Ocean. Sci.* 9 (4), 705–738.
- Malavieille, J., Lallemand, S., Dominguez, S., Deschamps, A., Lu, C.-Y., Liu, C.-S., Schnurle, P., Crew, A.S., 2002. Arc-continent collision in Taiwan: new marine observations and tectonic evolution. *Geol. Soc. Amer. Special Paper* 358, 187–211.
- McIntosh, K., Nakamura, Y., 1998. Crustal structure beneath the Nanao forearc basin from TAICRUST MCS/OBS Line 14. *Terr. Atmos. Ocean. Sci.* 9 (3), 345–362.
- McIntosh, K., Yosio Nakamura, T., Wang, T.-K., Shih, R.-C.A.C., Liu, C.-S., 2005. Crustal-scale seismic profiles across Taiwan and the western Philippine Sea. *Tectonophysics* 401, 23–54.
- Rau, R.-J., Wu, F.T., 1995. Tomographic imaging of lithospheric structures under Taiwan. *Earth Planet. Sci. Lett.* 133, 517–532.
- Schnurle, P., Liu, C.-S., Lallemand, S., Reed, D., 1998. Structural insight into the south Ryukyu margin: effects of the subducting Gagua Ridge. *Tectonophysics* 288, 237–250.
- Sibuet, J.-C., Hsu, S.-K., 1997. Geodynamics of Taiwan arc–arc collision. *Tectonophysics* 274, 221–251.
- Sibuet, J.C., Hsu, S.-K., Shyu, C.-T., Liu, C.-S., 1995. Structural and kinematic evolutions of the Okinawa Trough back-arc basin. In: Taylor, B. (Ed.), *Backarc Basins: Tectonics and Magmatism*. Plenum Press, New York, pp. 343–379.
- Sibuet, J.-C., Deffontaines, B., Hsu, S.-K., Thureau, N., Le Formal, J.P., Liu, C.-S., Party, T.A.C.T., 1998. Okinawa Trough back-arc basin: early tectonic and magmatic evolution. *J. Geophys. Res.* 103, 30245–30267.
- Suppe, J., 1981. Mechanics of mountain building in Taiwan. *Mem. Geol. Soc. China* 4, 67–89.
- Teng, L.S., Lee, C., Tsai, Y., Hsiao, L.-Y., 2000. Slab breakoff as a mechanism for flipping of subduction polarity in Taiwan. *Geology* 28 (2), 155–158.
- Tsai, Y.-B., 1985. A study of disastrous earthquakes in Taiwan. *Bull. Inst. Earth Sci. Acad. Sin.* 5, 1–44.
- Wang, J.-H., Kuo, H.-C., 1995. A catalogue of Ms 7 Taiwan Earthquakes (1900–1994). *J. Geol. Soc. China* 38 (2), 95–106.
- Wang, T.-K., Chiang, C.-H., 1998. Imaging of arc–arc collision in the Ryukyu forearc region offshore Hualien from TAICRUST OBS line 16. *Terr. Atmos. Ocean. Sci.* 9 (3), 329–344.
- Wang, T.-K., Lin, S.-F., Liu, C.-S., Wang, C.-S., 2004. Crustal structure of the southernmost Ryukyu subduction zone: OBS, MCS and gravity modelling. *Geophys. J. Int.* 157, 147–163.
- Wu, F.T., Rau, R.-J., Salzberg, D., 1997. Taiwan orogeny: thin-skinned or lithospheric collision? *Tectonophysics* 274 (1–3), 191–220.
- Yu, S.-B., Chen, H.-Y., Kuo, L.-C., 1997. Velocity field of GPS stations in the Taiwan area. *Tectonophysics* 274, 41–59.
- Zhou, H.-W., 1994. Rapid three-dimensional hypocentral determination using a master station method. *J. Geophys. Res.* 99 (B8), 15439–15455.